The EMBO Journal (2012) 31, 829–841 | © 2012 European Molecular Biology Organization | All Rights Reserved 0261-4189/12
www.embojournal.org

THE EMBO JOURNAL

CSPα knockout causes neurodegeneration by impairing SNAP-25 function

Manu Sharma[1,2,*], Jacqueline Burré[1,2], Peter Bronk[2,3], Yingsha Zhang[1,2], Wei Xu[1] and Thomas C Südhof[1,2,*]

[1]Department of Molecular and Cellular Physiology, Howard Hughes Medical Institute, Stanford University, Stanford, CA, USA and [2]Department of Neuroscience and Molecular Genetics, Howard Hughes Medical Institute, UT Southwestern Medical Center, Dallas, TX, USA

At a synapse, the synaptic vesicle protein cysteine-string protein-α (CSPα) functions as a co-chaperone for the SNARE protein SNAP-25. Knockout (KO) of CSPα causes fulminant neurodegeneration that is rescued by α-synuclein overexpression. The CSPα KO decreases SNAP-25 levels and impairs SNARE-complex assembly; only the latter but not the former is reversed by α-synuclein. Thus, the question arises whether the CSPα KO phenotype is due to decreased SNAP-25 function that then causes neurodegeneration, or due to the dysfunction of multiple as-yet uncharacterized CSPα targets. Here, we demonstrate that decreasing SNAP-25 levels in CSPα KO mice by either KO or knockdown of SNAP-25 aggravated their phenotype. Conversely, increasing SNAP-25 levels by overexpression rescued their phenotype. Inactive SNAP-25 mutants were unable to rescue, showing that the rescue was specific. Under all conditions, the neurodegenerative phenotype precisely correlated with SNARE-complex assembly, indicating that impaired SNARE-complex assembly due to decreased SNAP-25 levels is the ultimate correlate of neurodegeneration. Our findings suggest that the neurodegeneration in CSPα KO mice is primarily produced by defective SNAP-25 function, which causes neurodegeneration by impairing SNARE-complex assembly.

The EMBO Journal (2012) **31,** 829–841. doi:10.1038/emboj.2011.467; Published online 20 December 2011
Subject Categories: membranes & transport; neuroscience
Keywords: CSPα; neurodegeneration; SNAP-25; SNARE complex; synapse

Introduction

Cysteine-string protein-α (CSPα) is a synaptic vesicle protein (Buchner and Gundersen, 1997; Chamberlain and Burgoyne, 2000; Zinsmaier and Bronk, 2001) that contains a DnaJ-domain characteristic of co-chaperones, and forms a catalytically active chaperone complex with the DnaK-domain protein Hsc70 and the tetratricopeptide-repeat protein SGT (Chamberlain and Burgoyne, 1997; Tobaben *et al*, 2001). Deletion mutants of CSPα in Drosophila exhibit a temperature-sensitive phenotype that consists of neurodegeneration and synaptic dysfunction (Umbach *et al*, 1994; Zinsmaier *et al*, 1994). Knockout (KO) of CSPα in mice produces no immediately apparent phenotype at birth, but causes progressive neurodegeneration with paralysis and death at 2–4 months of age (Fernandez-Chacon *et al*, 2004). Experiments in the calyx of Held synapse that allows examination of presynaptic function at high resolution (Schneggenburger and Forsythe, 2006) revealed that at postnatal day 11 (P11), no impairment in synaptic function or neurodegeneration was detectable in CSPα KO mice (Fernandez-Chacon *et al*, 2004). After P20, however, significant impairments in synaptic transmission and massive neurodegeneration were evident (Fernandez-Chacon *et al*, 2004). Highly active neurons appear to be preferentially affected by neurodegeneration in CSPα KO mice, suggesting that the neurodegeneration is activity dependent (Garcia-Junco-Clemente *et al*, 2010). Similar to the KO mice, heterozygous mutations in the CSPα gene in humans cause autosomal-dominant adult-onset neuronal ceroid lipofuscinosis, a neurodegenerative disorder characterized by lysosomal accumulation of misfolded proteins (Nosková *et al*, 2011).

Biochemically, CSPα KO mice exhibit an ∼40% decrease in SNAP-25 levels and an ∼50% reduction in SNARE-complex assembly as measured in solubilized brain lysates (Chandra *et al*, 2005; Sharma *et al*, 2011). The decrease in SNAP-25 in CSPα KO mice is caused by increased ubiquitination and degradation of SNAP-25 (Sharma *et al*, 2011); this phenotype is temperature-sensitive, accounting for the temperature sensitivity of the Drosophila CSPα mutants (Umbach *et al*, 1994; Zinsmaier *et al*, 1994). Moreover, the purified CSPα/Hsc70/SGT chaperone complex prevented misfolding of purified SNAP-25 *in vitro* in an ATP-dependent manner, demonstrating in a reconstituted system that CSPα functions as a co-chaperone for SNAP-25 folding (Sharma *et al*, 2011).

However, these findings raised important new questions that are central for a molecular understanding of CSPα and of neurodegeneration. First, given that chaperones typically have many targets, is SNAP-25 the major substrate of the co-chaperone CSPα, or just one of many? Second, does the loss of functional SNAP-25 in CSPα KO mice cause the observed impairment in SNARE-complex assembly? Third, does the impairment in SNARE-complex assembly in turn produce neurodegeneration in CSPα KO mice, or are their SNARE-complex assembly deficits and their neurodegeneration separate downstream consequences of the complex action of CSPα on multiple targets?

The fact that overexpression of α-synuclein rescues the neurodegeneration of CSPα KO mice and reverses their SNARE-complex assembly deficit, but does not ameliorate their decrease in SNAP-25 levels (Chandra *et al*, 2005; Burre *et al*, 2010), already shed light onto these questions, but did

*Corresponding author. M Sharma or TC Südhof, Department of Molecular and Cellular Physiology, Howard Hughes Medical Institute, Stanford University, 265 Campus Drive, Stanford, CA 94305-5543, USA. Tel.: +1 650 721 1421; Fax: +1 650 498 4585;
E-mail: sharma11@stanford.edu or tcs1@stanford.edu
[3]Present address: Department of Biology, Brandeis University, 415 South Street, Waltham, MA 02454-9110, USA

Received: 27 July 2011; accepted: 28 November 2011; published online: 20 December 2011

not answer them. Specifically, α-synuclein rescues the SNARE-complex assembly deficit in CSPα KO mice by acting as a non-enzymatic chaperone for SNARE-complex assembly (Burre *et al*, 2010). Since in this activity α-synuclein rescues both the SNARE-complex assembly deficit and the neurodegeneration of CSPα KO mice, this observation supports the notion that the decrease in SNARE-complex assembly was the sole cause of neurodegeneration in CSPα KO mice. However, this result does not reveal whether the decrease in SNAP-25 levels in CSPα KO mice actually causes their impairment in SNARE-complex assembly, nor does it exclude alternative hypotheses for the genesis of the neurodegeneration. For example, it is possible that the impairment in SNARE-complex assembly in CSPα KO mice and the rescue of this impairment by α-synuclein are due to multiple indirect effects of these proteins. The CSPα KO could generate a toxic protein product, such as a protein aggregate or a misfolded protein, which might cause neurodegeneration but be neutralized by the non-specific surfactant-like activity of α-synuclein. The mechanism of neurodegeneration in CSPα KO mice is an important question not only because it sheds light onto the function of the evolutionarily ancient CSPα-chaperone system, but also because few neurodegenerative pathways have been defined at the molecular level. Understanding how precisely one form of neurodegeneration occurs may offer insights into neurodegenerative mechanisms in general.

Here, we have addressed these questions using a combination of genetic, molecular, and cell biological techniques, and tested the *in vivo* significance of SNAP-25 chaperoning by CSPα. Our data reveal that the SNARE-complex assembly impairment and the neurodegeneration in CSPα KO mice can be fully accounted for by the loss of functional SNAP-25 in these mice. This result suggests that SNAP-25 is the major substrate of the CSPα co-chaperone activity, and that the SNARE-complex assembly deficit is the predominant cause of neurodegeneration in CSPα KO mice. We propose a model whereby the distinct chaperone activities of CSPα and α-synuclein are required to maintain SNARE-protein function during continuous neurotransmitter release reactions. According to this model, neurodegeneration ensues in the absence of SNARE-complex chaperoning because of an imbalance between reactive SNARE proteins, not because of a change in neurotransmitter release. Thus, neurodegeneration caused by the CSPα KO may provide a paradigm for a more general role of presynaptic membrane traffic in neurodegeneration.

Results

Genetic decrease in SNAP-25 levels aggravates the CSPα KO phenotype

CSPα KO mice exhibit a decrease in SNAP-25 levels and in SNARE-complex assembly as early as postnatal day 5 (P5), long before neurodegeneration becomes apparent (Supplementary Figure S1A–D; Chandra *et al*, 2005; Sharma *et al*, 2011). As a first step towards determining whether neurodegeneration in CSPα KO mice is due to the loss of functional SNAP-25 resulting in impaired SNARE-complex assembly, we crossed CSPα KO mice (Fernandez-Chacon *et al*, 2004) with SNAP-25 KO mice (Washbourne *et al*, 2002). Heterozygous deletion of SNAP-25 by itself did not impair motor coordination or survival (Figure 1A–C; Supplementary Figure S1E). However, heterozygous deletion of SNAP-25 on top of the CSPα KO dramatically aggravated the motor deficits of CSPα KO mice, and decreased the survival time of CSPα KO mice ∼2-fold (note that homozygous SNAP-25 KO mice die at birth, and thus could not be analysed (Washbourne *et al*, 2002)).

We next examined the effect of the combination of SNAP-25 and CSPα KO alleles on SNAP-25 levels. In addition, we probed 25 other proteins with functions related to synaptic vesicle exo- and endocytosis in order to address the possibility that CSPα is a co-chaperone for other proteins. Furthermore, we also examined in these experiments CSPα KO mice in which the neurodegeneration was rescued by transgenic overexpression of α-synuclein using transgenic α-synuclein mice with wild-type (WT) CSPα expression as a control; testing these mice allowed us to differentiate between effects induced by a loss of SNAP-25 versus an impairment of SNARE-complex assembly versus an overexpression of α-synuclein. Using quantitative immunoblotting with ^{125}I-labelled secondary antibodies (Rosahl *et al*, 1995) to accurately determine protein levels, we found that heterozygous SNAP-25 KO mice exhibited an ∼40% decrease in SNAP-25 protein levels (Figure 1D), corresponding to the decrease in SNAP-25 mRNA levels (Supplementary Figure S1F). CSPα KO exhibited a similar decrease in SNAP-25 protein levels (Figure 1D) but not in mRNA levels, consistent with the increased degradation of SNAP-25 (Sharma *et al*, 2011). SNAP-25 protein levels were further decreased in the compound SNAP-25/CSPα mutants (Figure 1D). Besides SNAP-25, Hsc70 was decreased whenever CSPα was deleted, independent of neurodegeneration, showing that the Hsc70

Figure 1 Genetic reduction in SNAP-25 levels accelerates mortality of CSPα KO mice and decreases SNARE-complex assembly. (**A**) Images of representative WT mice, CSPα KO mice ($CSP^{-/-}$), heterozygous CSPα KO/heterozygous SNAP-25 KO mice ($CSP^{+/-}SNAP\text{-}25^{+/-}$), and homozygous CSPα KO/heterozygous SNAP-25 KO mice ($CSP^{-/-}SNAP\text{-}25^{+/-}$) at 30 days of age (P30). (**B**) Paralysis, as a neuromuscular sign of motor neuron degeneration, was recorded in mice of the indicated genotypes as a function of age (shown as the percentage of mice that uprighted in <5 s when placed on the side). $CSP^{-/-}SNAP\text{-}25^{+/-}$ mice were paralyzed significantly earlier than $CSP^{-/-}$ mice containing two WT SNAP-25 alleles ($n=9$–13 mice; $^{***}P<0.001$ by Mantel–Cox test). (**C**) Survival of littermate mice with the indicated genotypes as a function of age. In comparison, $CSP^{-/-}SNAP\text{-}25^{+/-}$ mice perish significantly earlier than $CSP^{-/-}$ mice ($n=9$–13 mice; $^{***}P<0.001$ by Mantel–Cox test). For a survival study including non-littermate mice, see Supplementary Figure S1E. (**D**, **E**) Protein (**D**) and SNARE-complex levels (**E**) in the brains from six different genotypes of mice at P20: WT, $SNAP\text{-}25^{+/-}$, $CSP^{-/-}$, $CSP^{-/-}SNAP\text{-}25^{+/-}$, transgenic α-synuclein (tSyn), and tSyn/$CSP^{-/-}$. (**D**) Representative immunoblots (left) and protein quantitations (right), obtained using ^{125}I-labelled secondary antibodies and normalized to GDI as internal standard. (**E**) SNARE-complex measurements in the same samples using co-immunoprecipitation of SNARE proteins (top, representative immunoblots; bottom, quantitations). Recovered protein (relative to the input) was normalized to the immunoprecipitated protein and then to WT levels ($n=4$ mice). Protein levels were measured by quantitative immunoblotting using ^{125}I-labelled secondary antibodies. Data shown are mean values ± s.e.m.; $^{*}P<0.05$; $^{**}P<0.01$; $^{***}P<0.001$ (assessed using Mantel–Cox (**B**, **C**) or Student's *t*-test (**D**, **E**), comparing each test condition to the control analysed in the same experiment). Figure source data can be found in Supplementary data.

decrease is not an indirect effect of neurodegeneration. In contrast, GFAP was increased and tau was decreased whenever there was neurodegeneration, indicating that their changes were caused by the neurodegeneration. α-Synuclein, finally, was increased in the transgenic mice as expected. No other protein tested, especially not proteins involved in exo- and endocytosis such as synaptotagmin, synaptophysin, dynamin, or AP180, exhibited a detectable change (Figure 1D; Supplementary Figure S1G).

To correlate SNAP-25 protein levels with SNARE-complex assembly, we next measured SNARE-complex formation in the brain homogenates from the various mice. Mice hetero-

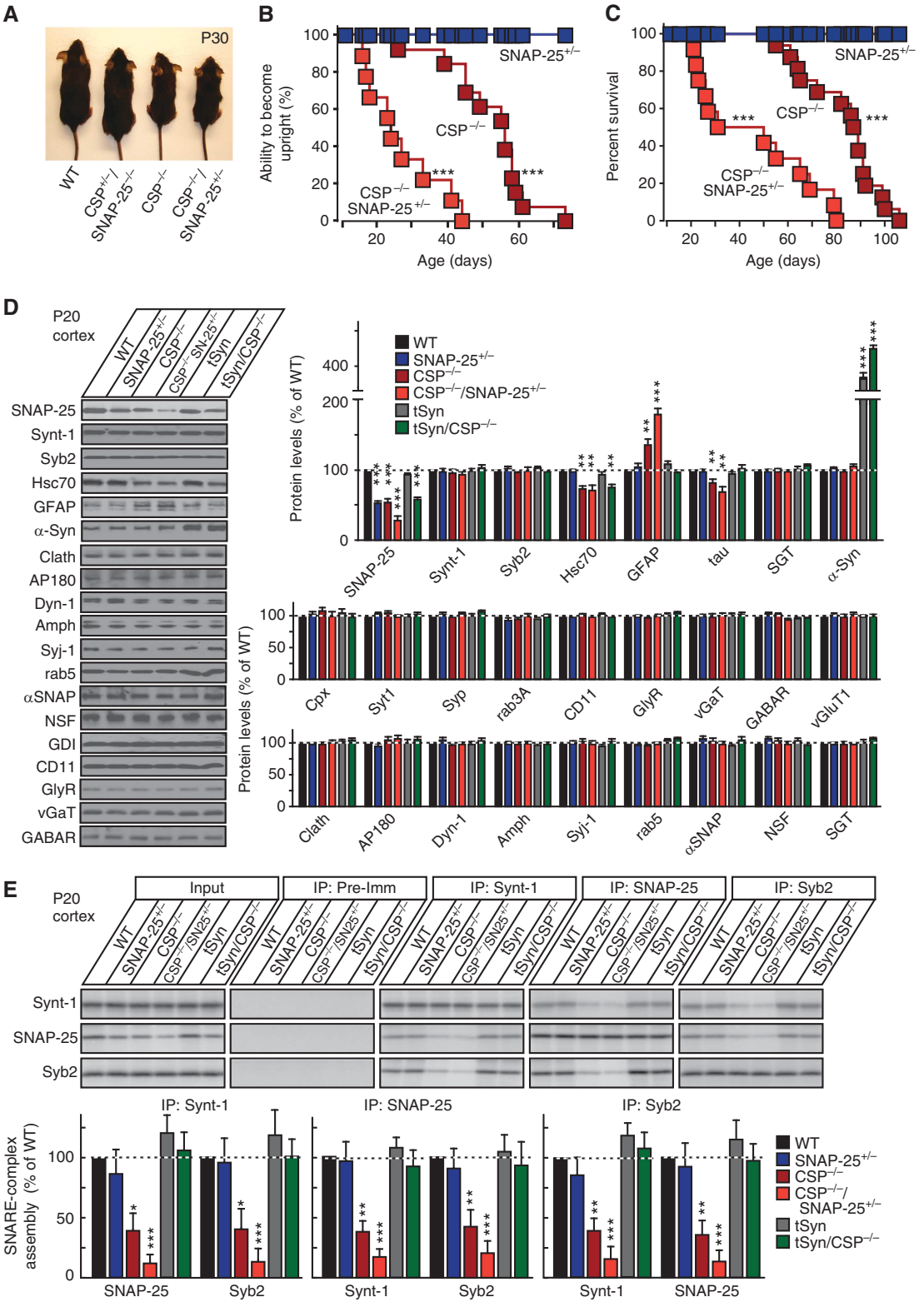

zygous for the SNAP-25 KO exhibited no change in SNARE-complex assembly, but heterozygous KO of SNAP-25 dramatically aggravated the SNARE-complex assembly deficit present in CSPα KO mice (Figure 1E; Supplementary Figure S1H and I). Transgenic α-synuclein, in contrast, rescued the SNARE-complex assembly deficit as described previously (Chandra *et al*, 2005). At first glance, it may appear puzzling that similar apparent decreases in total SNAP-25 levels lead to impaired SNARE-complex assembly and to lethal neurodegeneration in homozygous CSPα KO mice but not in heterozygous SNAP-25 KO mice. However, the remaining SNAP-25 in the CSPα KO mice is likely largely misfolded and dysfunctional (Sharma *et al*, 2011); the heterozygous SNAP-25 KO thus further decreases SNARE-complex assembly in CSPα KO mice because it halves the levels of the little remaining functionally active SNAP-25.

Large decreases in SNAP-25 levels by themselves do not cause a major impairment in synaptic transmission

The worsening of the CSPα KO phenotype by heterozygous KO of SNAP-25 supports the notion that the CSPα KO phenotype is due to a loss of functional SNAP-25, resulting in impaired SNARE-complex assembly. Yet, the constitutive nature of the SNAP-25 KO and its uniform presence in all cells of the mutant mice limit the interpretation of these experiments. Thus, we generated a short-hairpin RNA (shRNA) that when expressed by a lentivirus in cultured neurons, decreased the endogenous SNAP-25 mRNA by ∼90% (Figure 2A) and the endogenous SNAP-25 protein by >80% (Figure 2B). Electrophysiological recordings of inhibitory postsynaptic currents (IPSCs) from SNAP-25 knockdown (KD) neurons revealed that despite the loss of most SNAP-25, neurotransmitter release induced by isolated action potentials (Figure 2C–E) was not detectably altered. Even a short train of action potentials applied at 10 Hz did not uncover a significant deficit in SNAP-25 deficient neurons (Supplementary Figure S2A–C), and only a train of 100 action potentials applied at 10 Hz elicited a minor but significant decrease in synaptic charge transfer (Figure 2F–H). Moreover, we observed no change in the readily releasable pool of vesicles measured using hypertonic sucrose (Figure 2I and J),

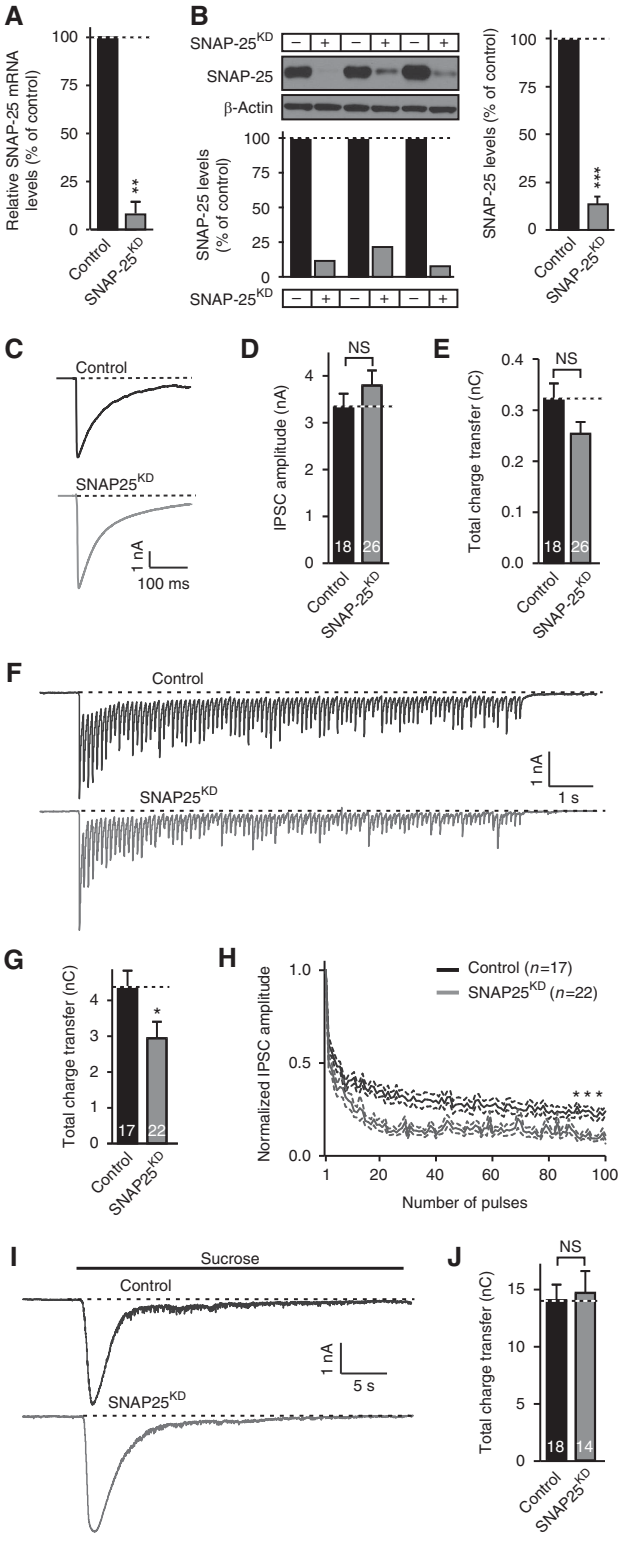

Figure 2 SNAP-25 KD in WT neurons does not dramatically decrease synaptic transmission. (**A**, **B**) Characterization of the SNAP-25 KD efficiency using mRNA (**A**) and protein measurements (**B**). Cultured cortical neurons from WT mice were infected with lentiviruses expressing SNAP-25 shRNA and mCherry (SNAP-25^{KD}) or mCherry alone (control) at 5 DIV, and analysed at DIV14 by quantitative RT–PCR to measure SNAP-25 mRNA levels (**A**, normalized to GAPDH mRNA levels) or by quantitative immunoblotting to measure SNAP-25 protein levels (**B**) normalized to β-actin; left shows immunoblots and protein levels in each culture; right, summary graph of quantitations. (**C**, **E**) Effect of the SNAP-25 KD on synaptic transmission triggered by isolated action potentials in cultured cortical neurons obtained as described above. (**C**) Representative traces of inhibitory postsynaptic synaptic currents (IPSC); (**D**) summary graphs of the IPSC amplitude; (**E**), summary graphs of the IPSC charge transfer. (**F**, **H**) Same as (**C**–**E**), except that IPSCs evoked by stimulus trains (100 stimuli applied at 10 Hz) were examined. (**F**) Representative traces; (**G**) summary graphs of the total charge transfer induced by the train; (**H**) normalized amplitudes of individual synchronous IPSCs to monitor synaptic depression. For shorter 10 Hz stimulus trains, see Supplementary Figure S2. (**I**, **J**) Same as (**C**–**E**), except that IPSCs were evoked by a 30-s application of hypertonic sucrose (0.5 M). Representative traces (**I**) and summary graphs of the total charge transfer (**J**) are shown. Data shown are mean values ± s.e.m.; $n=3$ independent cultures; numbers shown in panels (**C**–**J**) indicate the number of neurons analysed. NS, not significant ($P>0.05$); *$P<0.05$; **$P<0.01$; ***$P<0.001$ (using Student's *t*-test (**B**, **D**, **E**, **G**, **J**) or two-way repeated-measures ANOVA (**H**), comparing each test condition to the control analysed in the same experiment). Figure source data can be found in Supplementary data.

or in inhibitory (mIPSCs) and excitatory (mEPSCs) spontaneous release events (Supplementary Figure S2D–I).

Thus, a loss of the vast majority of SNAP-25 from neurons does not cause a major synaptic phenotype, as opposed to a complete loss of SNAP-25 in KO mice that blocks synaptic transmission (Washbourne *et al*, 2002; Bronk *et al*, 2007). This surprising result suggests that the small amount of reserve SNAP-25 protein remaining in KD neurons is largely sufficient for full presynaptic function. This conclusion is consistent with the finding that CSPα KO and αβγ-synuclein triple KO neurons also do not exhibit a significant release phenotype prior to the onset of neurodegeneration (Fernandez-Chacon *et al*, 2004; Burre *et al*, 2010). The question thus arises, does the SNAP-25 KD accelerate neurodegeneration induced by the loss of CSPα?

Reduction in SNAP-25 levels increases neurodegeneration in CSPα KO mice

In the next set of experiments, we cultured neurons from littermate WT and heterozygous and homozygous CSPα KO mice, infected the neurons with control lentivirus or lentivirus expressing the SNAP-25 shRNA, and measured the levels of SNARE proteins after 14 days *in vitro* (DIV). As expected, the combination of the CSPα KO and the SNAP-25 KD decreased SNAP-25 levels below those observed with either manipulation alone, whereas the expression of other SNARE and synaptic proteins assayed was not altered (Figure 3A; Supplementary Figure S3). We then measured SNARE-complex assembly in the same samples by immunoblotting of SDS-resistant SNARE complexes (Figure 3B) and by immunoprecipitations (Figure 3C). Both methods showed that the SNAP-25 KD or the heterozygous CSPα KO alone did not significantly impair SNARE-complex assembly, whereas the combination of the heterozygous CSPα KO with the SNAP-25 KD decreased SNARE-complex assembly by ∼60%, indicating a synthetic effect. Moreover, addition of the SNAP-25 KD to the homozygous CSPα KO aggravated the SNARE-complex assembly deficit in the latter, producing an ∼90% decrease in such assembly.

To explore whether the aggravation of the CSPα KO phenotype by the SNAP-25 KD in cultured neurons translates into increased neurodegeneration *in vivo*, we injected concentrated lentiviruses expressing the SNAP-25 shRNA and mCherry (as a marker), or mCherry alone, into the cortex of neonatal WT mice and of heterozygous and homozygous CSPα KO mice. Neonatal mice were stereotactically injected at P1, and their brains were analysed by immunofluorescence staining at P50 to measure neuron density, synapse density, and caspase-3 cleavage during apoptosis in areas infected by the lentiviruses (Figure 4). Comparisons of the uninjected and control-injected cortex of WT mice and of heterozygous and homozygous CSPα KO mice revealed that the homozygous CSPα KO caused an ∼50% reduction in the relative density of neurons (measured as the percentage of nuclei expressing the neuron-specific nuclear protein NeuN), an ∼40% reduction in synapse density (measured with the postsynaptic excitatory marker PSD95), an ∼70% increase in apoptosis (measured with cleaved caspase-3), while simultaneously producing massive astrogliosis (assayed by GFAP staining; Figure 4; Supplementary Figure S4). The heterozygous CSPα KO, conversely, had no effect on neuronal density, synapse density, or apoptosis.

We then analysed the effect of the control and SNAP-25 KD lentiviral infection on neuron numbers, synapse density, and apoptosis. Compared with the control, the SNAP-25 KD had no effect on neuron numbers, synapse density, or apoptosis in WT cortex, but caused a highly significant decrease in neuronal and synaptic density, as well as an increase in apoptosis, in the cortex of heterozygous CSPα KO mice (Figure 4). Furthermore, the SNAP-25 KD aggravated the decrease in neuron numbers and synapse density in homozygous CSPα KO mice, while increasing apoptosis in these mice. Thus, acute suppression of SNAP-25 expression induces neurodegeneration in heterozygous CSPα KO mice, and aggravates neurodegeneration in homozygous CSPα KO mice.

Increasing SNAP-25 levels rescues the CSPα KO phenotype

If the CSPα KO phenotype was primarily caused by a lack of SNAP-25 chaperoning, resulting in an impairment of SNARE-complex assembly, it should be possible to not only aggravate the CSPα KO phenotype by further decreasing the levels of SNAP-25, but also to rescue the CSPα KO phenotype by increasing the levels of SNAP-25. If, on the other hand, the CSPα KO phenotype resulted from the combined decrease in the functions of SNAP-25 and of other proteins, then a further decrease in SNAP-25 may still be able to aggravate the phenotype, but an increase in SNAP-25 should not be able to rescue the phenotype.

To address these hypotheses, we constructed lentiviruses expressing WT SNAP-25 N-terminally fused to GFP, or two truncation mutants of SNAP-25. The SNAP-25 truncation mutants were chosen to reflect the cleavage products of botulinum toxin A (residues 1–197) and botulinum toxin E (residues 1–180); both of these truncations impair SNAP-25 function in neurotransmitter release (Huang *et al*, 1998; Yang *et al*, 2000). In neurons, SNAP-25 is not specifically concentrated in presynaptic terminals, but is enriched in axons (Tao-Cheng *et al*, 2000). When expressed in cultured neurons from CSPα KO mice, the GFP-fusion proteins of WT SNAP-25 and of the two SNAP-25 truncation mutants exhibited the same localization, with a relative enrichment in axons and exclusion from dendrites as evidenced by their co-localization with synapsin and their lack of co-localization with the dendritic marker MAP2 (Figure 5A and B; Supplementary Figure S5A); moreover, WT and mutant SNAP-25 GFP-fusion proteins were expressed at similar levels (Figure 5C; Supplementary Figures S5B and S6B).

Strikingly, WT SNAP-25 increased SNARE-complex assembly by ∼200% in CSPα KO neurons, whereas the two truncation mutants of SNAP-25 had no effect (Figure 5D–F). In particular and different from a previous study (Yang *et al*, 2000), we detected no suppression of SNARE-complex assembly by the SNAP-25 1–180 truncation mutant. Moreover, we observed no significant changes in the levels of other proteins assayed upon GFP–SNAP-25 overexpression in CSPα KO neurons except for a slight increase in vGaT levels (Supplementary Figure S5C).

Finally, we examined the *in vivo* effects of SNAP-25 overexpression on neurodegeneration induced by the CSPα KO, using stereotactic injections of concentrated lentiviruses expressing SNAP-25 into mouse brains. Mice were injected at P1, and analysed at P50. Examination of neuron density,

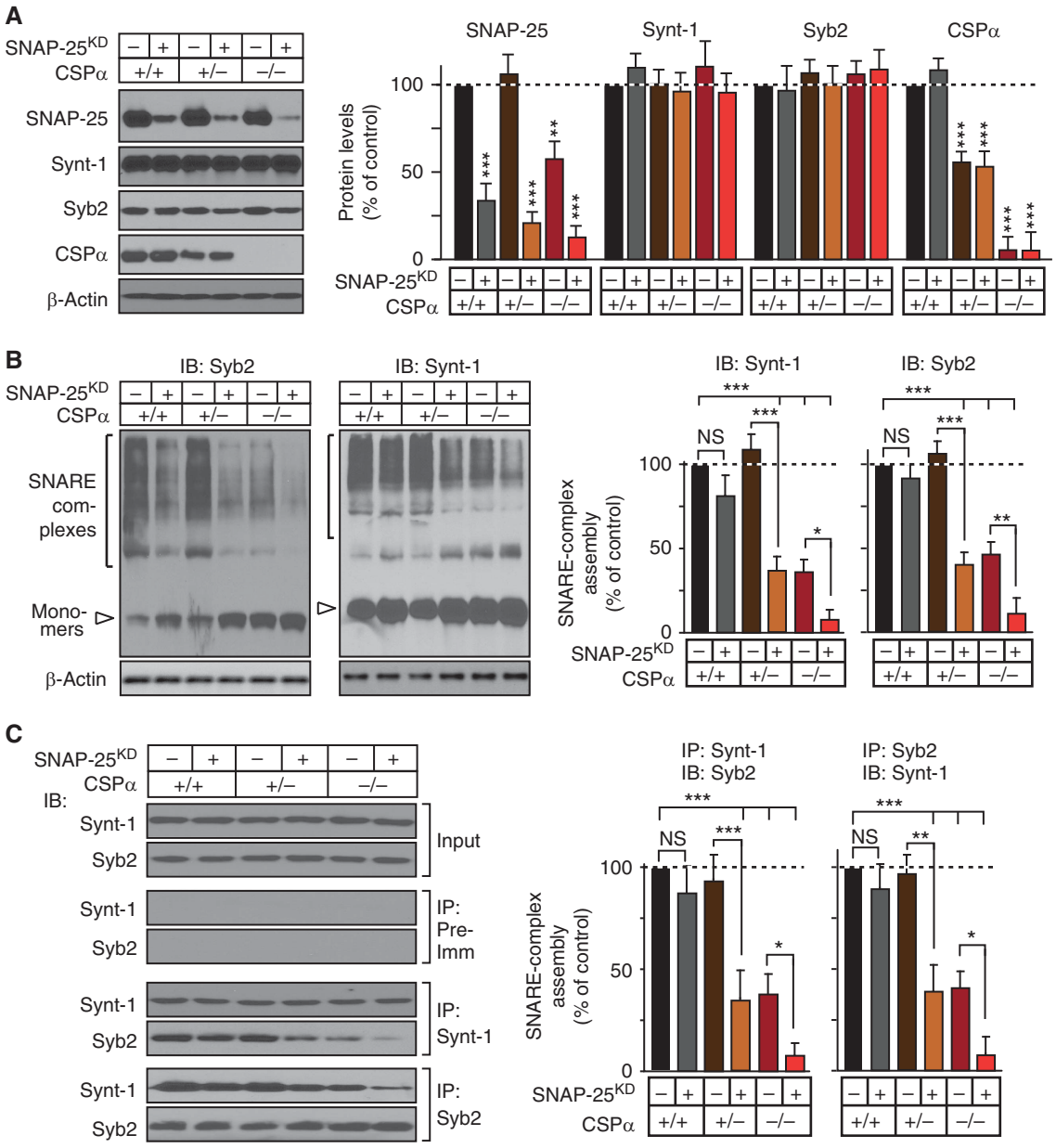

Figure 3 SNAP-25 KD reduces SNARE-complex assembly. Cortical neurons cultured from WT mice and heterozygous and homozygous CSPα KO mice were infected with lentiviruses expressing the SNAP-25 shRNA and mCherry (SNAP-25^{KD}) or mCherry alone at DIV5, and SNAP-25 protein levels and SNARE-complex assembly were measured at DIV14. (**A**) SNARE and CSPα protein levels measured in cortical cultures from WT, heterozygous CSPα KO (CSPα$^{+/-}$), and homozygous CSPα KO (CSP$^{-/-}$) mice infected with lentiviruses expressing SNAP-25 shRNA and mCherry or mCherry alone, and normalized to β-actin (left, representative immunoblots; right, summary graph of protein levels). (**B**) SNARE-complex assembly in WT, CSPα$^{+/-}$, or CSP$^{-/-}$ neurons infected as above, quantitated as high molecular mass bands in Syb2 and Synt-1 immunoblots, and normalized to β-actin (left, representative immunoblots; right, SNARE-complex levels). (**C**) Cultured cortical neurons from WT, CSPα$^{+/-}$, and CSP$^{-/-}$ mice were infected as above, and lysates obtained at DIV14 were subjected to SNARE protein co-immunoprecipitation using Synt-1 or Syb2 antibodies, followed by immunoblotting to measure SNARE-complex assembly (left, representative immunoblots; right, quantitations). Recovered protein (relative to the input) was first normalized to the immunoprecipitated protein, and then to WT levels. Protein levels were measured by quantitative immunoblotting using ^{125}I-labelled secondary antibody. Data are shown as mean values ± s.e.m.;, $n = 3$ cultures; NS, not significant ($P > 0.05$); *$P < 0.05$; **$P < 0.01$; ***$P < 0.001$ (using Student's *t*-test, comparing each test condition to the control analysed in the same experiment). Figure source data can be found in Supplementary data.

synapse density, apoptosis, and astrogliosis revealed that the neurodegeneration associated with CSPα KO was largely reversed in the cortical area expressing WT SNAP-25 (Figure 6; Supplementary Figure S6). In contrast, no rescue of neurodegeneration was detected in areas expressing either GFP alone or either one of the two truncation mutants of SNAP-25.

Discussion

Previous studies revealed that KO of CSPα, a synaptic vesicle protein with a DnaJ-domain, decreases SNAP-25 levels, impairs SNARE-complex assembly, and produces neurodegeneration (Fernandez-Chacon *et al*, 2004; Chandra *et al*, 2005; Garcia-Junco-Clemente *et al*, 2010). Biochemically, CSPα acts

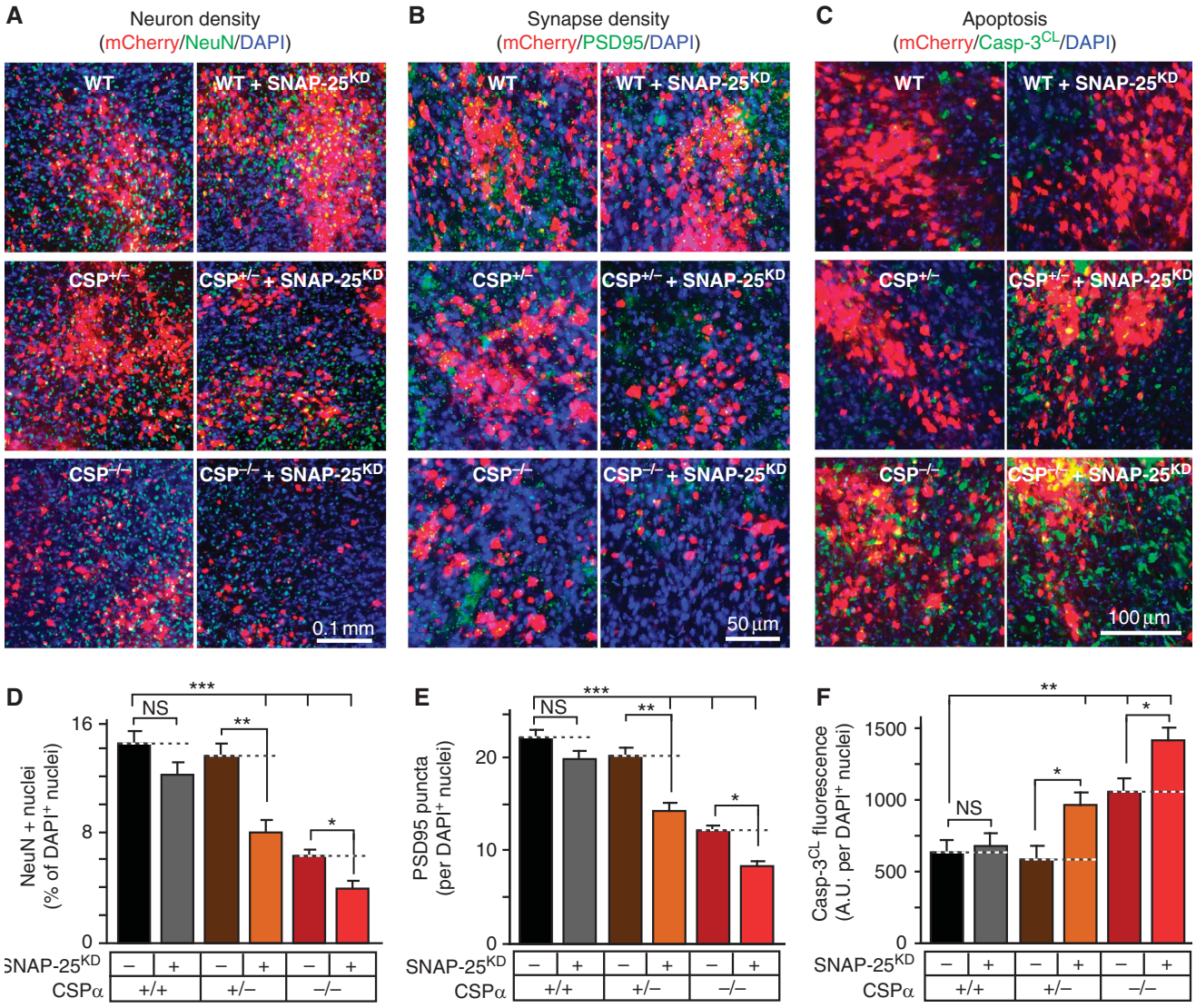

Figure 4 SNAP-25 KD aggravates neurodegeneration. (**A**–**F**) Effect of SNAP-25 KD on neurodegeneration was assessed in WT, heterozygous (CSPα$^{+/-}$), and homozygous CSPα KO (CSP$^{-/-}$) mouse brains. Stereotactic injections of lentiviruses at P1 in WT, CSPα$^{+/-}$, and CSP$^{-/-}$ mouse cortex were used to express mCherry as a control, or SNAP-25 shRNA with mCherry (SNAP-25^{KD}/mCherry). (**A**, **D**) At P50, neuron density in the infected areas was quantitated by immunostaining for NeuN (green), and visualizing DAPI (blue) and mCherry (red). (**B**, **E**) Synapse density in the infected areas was quantitated by immunostaining for PSD95 (green), and visualizing DAPI (blue) and mCherry (red). (**C**, **F**) Apoptosis in the infected areas was quantitated by immunostaining for cleaved caspase-3 (Casp-3^{CL}; green), and visualizing DAPI (blue) and mCherry (red). See Supplementary Figure S4B, D, and H for individual images. Data are shown as mean values ± s.e.m.; $n = 3$ mice, 10 sections for each; NS, not significant ($P > 0.05$); *$P < 0.05$; **$P < 0.01$; ***$P < 0.001$ (using Student's *t*-test, comparing each test condition to the control analysed in the same experiment).

as a co-chaperone that maintains the function of SNAP-25 in presynaptic terminals during repeated rounds of exo- and endocytosis involving SNARE-complex assembly and disassembly (Tobaben *et al*, 2001; Sharma *et al* 2011). Collectively, these results identified CSPα as a novel SNARE chaperone, but raised major new questions, which we have now tried to address. Is SNAP-25 the major substrate of the co-chaperone CSPα, or just one of many? Is it the loss of SNAP-25 function that impairs SNARE-complex assembly in CSPα KO mice, or do multiple parallel changes cause this impairment? Does the impairment in SNARE-complex assembly in turn cause neurodegeneration, or are the SNARE-complex assembly deficits and neurodegeneration in CSPα KO mice separate downstream effects of the loss of multiple actions of CSPα?

In trying to address these questions, we made four principal observations:

1. Deletion of CSPα selectively alters SNAP-25 levels and SNARE-complex assembly without significantly affecting the levels of other synaptic proteins.
2. Genetic decrease in SNAP-25 expression in heterozygous SNAP-25 KO mice does not in itself produce neurodegeneration, but dramatically aggravates the SNARE-complex assembly deficit and neurodegeneration of CSPα KO mice.
3. shRNA-dependent KD of SNAP-25 in CSPα KO mice similarly decreases SNARE-complex assembly and increases neurodegeneration.
4. Overexpression of WT but not C-terminally truncated SNAP-25 rescues the CSPα KO phenotype, both in terms

of the decrease in SNARE-complex assembly and in terms of the neurodegeneration.

These data strongly argue that the CSPα KO phenotype is largely if not exclusively caused by loss of CSPα-dependent chaperoning of SNAP-25, which leads to impaired SNARE-complex assembly that in turn then causes neurodegeneration. To test this hypothesis further, we plotted the number of neurons and the density of synapses observed in the brain sections as a function of the biochemically measured SNARE-complex assembly efficiency (Figure 7A). The plot shows that neuron numbers and synapse density (which in turn are a function of the degree of neurodegeneration) directly correlate with SNARE-complex assembly. Since the SNARE-complex assembly deficit precedes the neurodegeneration in CSPα KO mice, these data indicate that this deficit causes the neurodegeneration.

Although our data do not exclude the possibility that CSPα acts on other substrates besides SNAP-25, they show that the major features of the CSPα KO phenotype can be accounted for by the function of CSPα as a SNAP-25 chaperone. As a result, we propose a model whereby the neurodegeneration induced by the CSPα KO arises from an impairment in SNARE-complex assembly that in turn is the result of the

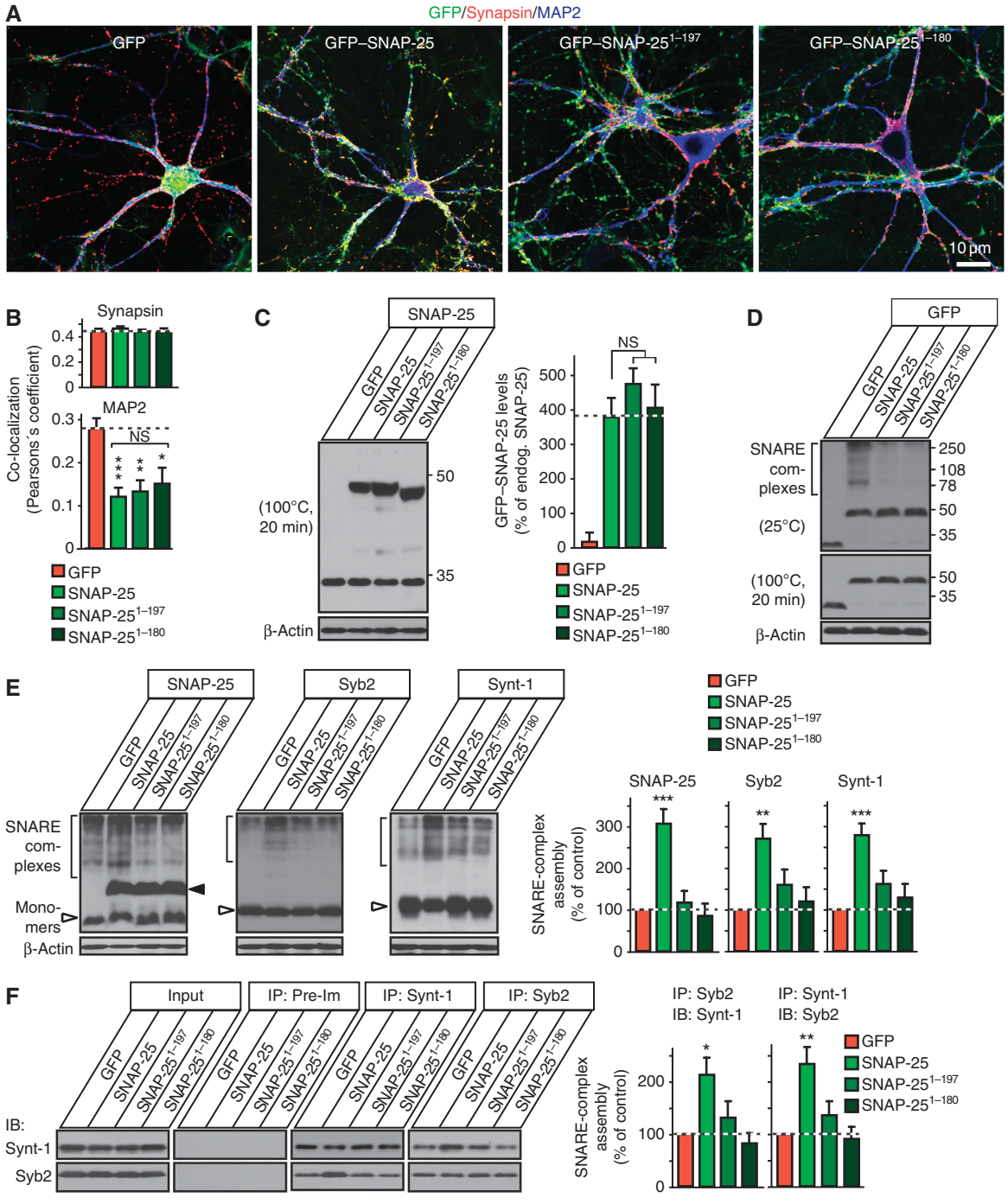

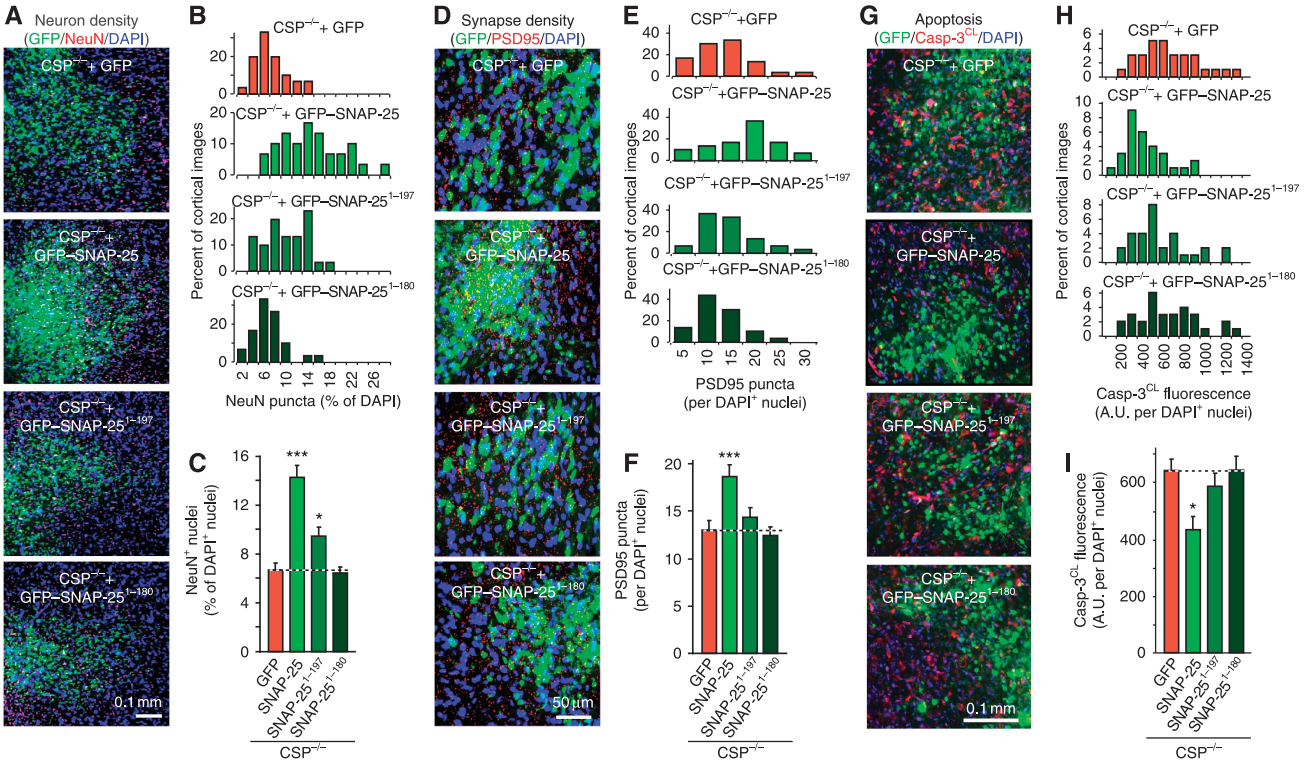

Figure 6 SNAP-25 overexpression rescues neurodegeneration in CSPα KO mice. (**A–C**) GFP–SNAP-25 expression reverts neuron loss in $CSP^{-/-}$ mice. Lentiviruses expressing GFP alone, GFP–SNAP-25 WT, or truncated versions (GFP–SNAP-25^{1-197} and GFP–SNAP-25^{1-180}) were injected into the cortex of littermate newborn $CSP^{-/-}$ mice. Mice were analysed at P50 by immunocytochemistry for NeuN puncta relative to DAPI puncta in the injected areas. (**A**) Representative merged images of GFP (green), NeuN (red), and DAPI signals (blue; for individual images, see Supplementary Figure S5). (**B**) Distribution of NeuN puncta density as percent of DAPI and (**C**) summary graph. (**D–F**) SNAP-25 overexpression rescues the reduction in synapse density in $CSP^{-/-}$ mouse cortex. (**D**) Following lentiviral expression of GFP alone, GFP–SNAP-25, GFP–SNAP-25^{1-197}, or GFP–SNAP-25^{1-180}, brain sections were immunostained for GFP (green), PSD95 (red), and DAPI (blue) at P50. PSD95 puncta were analysed as a function of DAPI puncta. (**E**) Distribution of PSD95 puncta as percent of DAPI and (**F**) summary graph. (**G–I**) SNAP-25 overexpression rescues the elevated apoptosis in $CSP^{-/-}$ mouse cortex. (**G**) Following lentiviral expression *in vivo* as above, the brain sections were immunostained for GFP (green), cleaved caspase-3 (Casp-3^{CL}; red), and DAPI (blue) at P50. Total Casp-3^{CL} positive pixels were analysed as a function of DAPI puncta. (**H**) Distribution of Casp-3^{CL} staining as percent of DAPI and (**I**) summary graph. See Supplementary Figure S6A for individual images. Data shown are mean values ± s.e.m.; $n = 3$ mice, 10 sections for each; $^{*}P < 0.05$; $^{***}P < 0.001$. Statistical significance was assessed by Student's *t*-test, comparing each test condition to the control analysed in the same experiment.

Figure 5 SNAP-25 overexpression increases SNARE-complex assembly in CSPα KO neurons. (**A**) Localization of GFP-tagged WT SNAP-25 (GFP–SNAP-25), and truncated SNAP-25 versions (GFP–SNAP-25^{1-197} and GFP–SNAP-25^{1-180}) in CSPα KO ($CSP^{-/-}$) neurons. Cultured cortical neurons from newborn $CSP^{-/-}$ mice were infected with lentiviruses expressing GFP alone or indicated GFP-tagged version of SNAP-25 at DIV7, and analysed by immunofluorescence at DIV14 (green, GFP; red, synapsin; blue, MAP2). For individual channels and quantitation of co-localization, see Supplementary Figure S5A. (**B**) Co-localization of GFP, GFP–SNAP-25, GFP–SNAP-25^{1-197}, and GFP–SNAP-25^{1-180} either with synaptic marker synapsin or with microtubule-associated protein MAP2 was quantitated using Pearson's coefficient. (**C**) Levels of GFP–SNAP-25, GFP–SNAP-25^{1-197}, and GFP–SNAP-25^{1-180} expression were measured from $CSP^{-/-}$ neurons infected as in (**A**). Neuronal lysates were boiled for 20 min to melt SNARE complexes and were immunoblotted for SNAP-25 and β-actin. Representative immunoblots (left) and quantitations normalized to β-actin as loading control (right). (**D**) GFP–SNAP-25 participates in SNARE-complex assembly. Representative immunoblots of non-boiled (top) and boiled samples (bottom) from cultured $CSP^{-/-}$ neurons infected as in (**A**). GFP–SNAP-25 WT but not its truncated versions are incorporated into SNARE-complexes, as indicated by high molecular mass bands specifically in GFP–SNAP-25 expressing cultures (top), which are melted by boiling for 20 min (bottom). (**E**) Effect of SNAP-25 overexpression in $CSP^{-/-}$ neurons on SNARE-complex assembly. In $CSP^{-/-}$ cultured neurons expressing GFP or indicated version of GFP–SNAP-25, SNARE complexes were separated as high molecular mass bands immunoreactive for SNAP-25, Syb2, and Synt-1 and quantitated with normalization to β-actin (loading control). (**F**) Effect of SNAP-25 overexpression in $CSP^{-/-}$ neurons on SNARE-complex assembly. $CSP^{-/-}$ cortical neuron cultures were infected with indicated lentiviruses as in (**A**). Lysates obtained on DIV14 were subjected to SNARE protein co-immunoprecipitation using Syb2 and Synt-1 antibodies, followed by immunoblotting to measure SNARE-complex assembly. Recovered protein (relative to the input) was first normalized to the immunoprecipitated protein, and then to GFP only expressing controls. Protein levels were determined using phosphor-imager analysis with ^{125}I-labelled secondary antibody. Data shown are mean values ± s.e.m.; $n = 4$ cultures; NS, not significant ($P > 0.05$); $^{*}P < 0.05$; $^{**}P < 0.01$; $^{***}P < 0.001$. Statistical significance was assessed by Student's *t*-test, comparing each test condition to the control analysed in the same experiment. Figure source data can be found in Supplementary data.

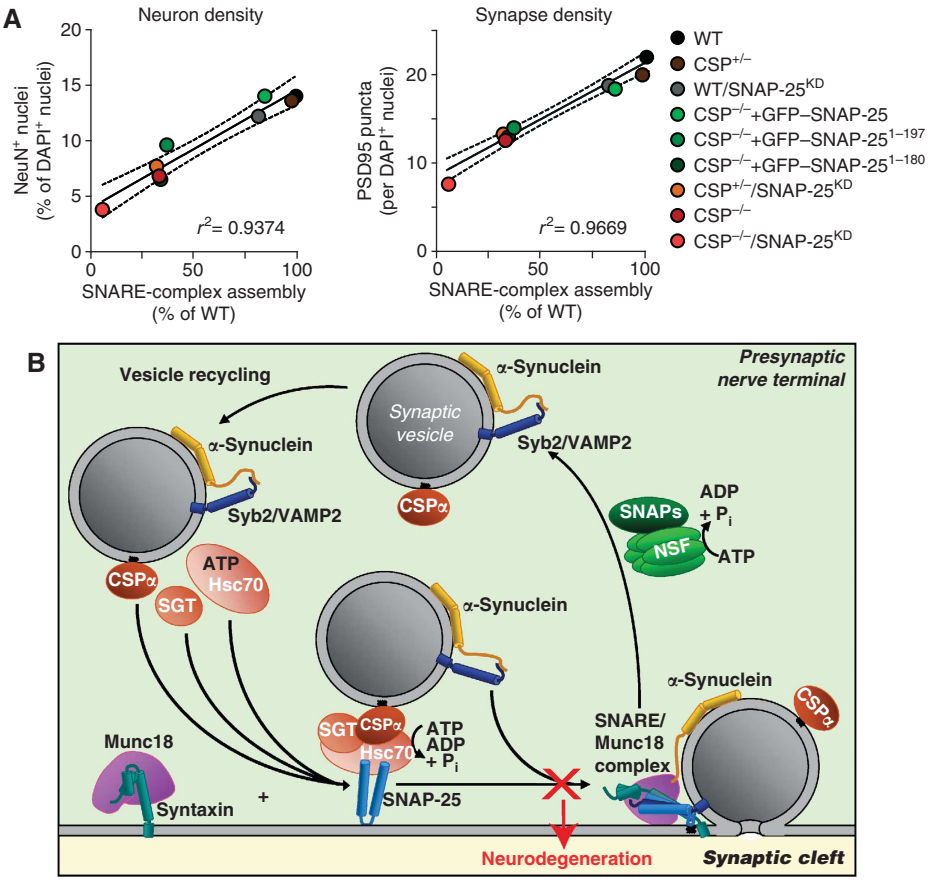

Figure 7 Correlation of SNARE-complex levels with neurodegeneration. (**A**) Linear relationship between SNARE-complex assembly and neuronal loss (left) or synapse loss (right). Dotted lines show 95% confidence interval. (**B**) Model depicting the presynaptic SNARE cycle. 'X' indicates the disruption of SNARE-complex assembly, which leads to neurodegeneration. VAMP2, vesicle-associated membrane protein 2; SNAP, soluble NSF attachment protein.

loss of SNAP-25 chaperoning (Figure 7B). With this model, we suggest that impaired SNARE-complex assembly does not cause neurodegeneration via a decrease in neurotransmitter release, but because the impairment in SNARE-complex assembly leads to an excess of reactive SNARE proteins that do not participate in SNARE complexes. Specifically, the loss of functional SNAP-25 in the CSPα KO mice results in a relative excess of syntaxin-1 (Synt-1) and synaptobrevin-2 (Syb2) over SNAP-25. As SNARE proteins, Synt-1 and Syb2 are highly reactive and may engage in inappropriate protein interactions that damage the nerve terminals, resulting in neurodegeneration.

Our model is supported by three major lines of evidence: First, the loss of functional SNAP-25 in CSPα KO mice is solely responsible for the neurodegeneration (Figures 1–6); second, the level of SNARE-complex assembly precisely correlates with neurodegeneration (Figure 7A); and third, the neurodegeneration in CSPα KO mice is rescued by α-synuclein overexpression (Chandra *et al*, 2005), which does not restore SNAP-25 levels, but directly enhances SNARE-complex assembly (Burre *et al*, 2010).

An alternative model could be that the loss of CSPα-dependent SNAP-25 chaperoning generates a toxic SNAP-25 conformer, which inhibits SNARE-complex formation and/or damages the nerve terminal. According to this scenario, chaperoning of SNAP-25 would still be sufficient in heterozygous CSPα KO mice to prevent neurodegeneration, and α-synuclein overexpression rescues the CSPα KO neurodegeneration because α-synuclein may conceivably detoxify this hypothetical SNAP-25 conformer. However, the fact that the SNAP-25 KD elicits a neurodegenerative phenotype in heterozygous CSPα KO mice and that SNAP-25 overexpression rescues the CSPα KO phenotype renders this second hypothesis unlikely.

Another, less-defined alternative model could be that CSPα may generally chaperone synaptic vesicle trafficking via acting on multiple targets, and that neurodegeneration develops in CSPα KO mice because of the cumulative effects of multiple trafficking defects. However, our finding that the CSPα KO phenotype can be selectively enhanced or alleviated by manipulations that decrease or increase SNAP-25 levels, respectively, strongly argues against this model. Moreover, the observation that CSPα KO mice do not exhibit a detectable synaptic transmission defect in the calyx of Held synapse before neurodegeneration occurs rules out this hypothesis (Fernandez-Chacon *et al*, 2004). In this respect, the finding that the impairment in SNARE-complex assembly in CSPα KO mice does not suffice to decrease synaptic transmission (Fernandez-Chacon *et al*, 2004) is consistent with our present data, showing that a large decrease in SNAP-25 levels induced by the SNAP-25 KD does not produce a major impairment in synaptic transmission (Figure 2). Together, these observations reveal an enormous functional reserve for SNARE proteins at the synapse, in agreement with the high expression levels of these proteins.

Does the neurodegenerative mechanism described here potentially apply to other forms of neurodegeneration, and is this mechanism relevant for human disease? Significant evidence points to a presynaptic locus in neurodegeneration in at least some cases of Alzheimer's and Parkinson's disease (Wishart *et al*, 2006; Kramer and Schulz-Schaeffer, 2007; Scheff *et al*, 2007). Moreover, the widespread involvement of α-synuclein in neurodegenerative disorders (Galvin *et al*, 2001) and the function of α-synuclein as a SNARE chaperone (Burre *et al*, 2010) generally support the notion that SNARE proteins may have a role in human neurodegeneration. Yet, at this point no direct evidence for a role of impaired SNARE-complex assembly in human neurodegeneration exists, whereas much evidence points to toxic protein fragments or conformers as causative agents in human neurodegeneration (Rubinsztein, 2006; Yankner *et al*, 2008). However, the 'toxic protein' hypothesis has not yet been confirmed for any neurodegenerative disorder. Moreover, the mechanism of neurodegeneration outlined here raises the possibility that these toxic agents could act by specifically interfering with SNARE-dependent presynaptic membrane traffic, including a loss of SNARE-protein function. For example, sequestration of α-synuclein into Lewy bodies is a hallmark of several neurodegenerative diseases (Galvin *et al*, 2001), and may decrease the levels of functional α-synuclein in the respective neuron. We hope that with the present description of a defined neurodegenerative pathway, a more concrete examination of these questions may now become possible.

Materials and methods

Mouse breeding experiments

CSPα KO mice were bred $CSP^{+/-}$ to $CSP^{+/-}$ as described (Fernandez-Chacon *et al*, 2004). For analysis of the effect of decreasing SNAP-25 levels on CSPα KO mice, we first generated compound heterozygous SNAP-25 KO mice (Washbourne *et al*, 2002)/CSPα KO mice. The *SNAP-25* and *CSPα* genes are both on mouse chromosome 2 (≈45 Mbp, or ≈24 cM apart); thus, any analysis of the effect of SNAP-25 heterozygosity on the CSPα KO phenotype requires the two mutant alleles to be on the same chromosome, which necessitated extensive crossings to obtain the required recombination and confirm it in subsequent breedings. We then bred SNAP-25/CSPα double heterozygous mice either to each other, or with CSPα heterozygous mice, and analysed the survival and biochemical properties of the resulting littermate offspring (note that since homozygous SNAP-25 KO mice are lethal (Washbourne *et al*, 2002), these were not present in the analysis). CSPα mice rescued by the transgenic expression of human α-synuclein (tSyn/$CSP^{-/-}$) (Chandra *et al*, 2005) were bred as tSyn/$CSP^{+/-}$ to $CSP^{+/-}$ in order to keep the transgene expression constant. The animal protocols used in this study, as well as the overall mouse and rat husbandry practices were approved by the respective Institutional Animal Care and Use Committees at UT Southwestern Medical Center and Stanford University.

Primary mouse cultured neurons

Mouse cortical neurons were cultured from newborn mice essentially as described (Tang *et al*, 2006; Maximov *et al*, 2007). Brain regions were dissected in ice-cold Hank's Balanced Salt Solution, dissociated by trypsinization (0.05% trypsin-EDTA, for 10 min at 37°C), triturated with a siliconized pipette, and plated (100 μl) onto a 12-mm coverslip (for immunofluorescence) or on 12-well plastic dishes, coated for at least 30 min with Matrigel (BD Biosciences). Plating medium (MEM (Gibco) supplemented with 5 g/l glucose, 0.2 g/l $NaHCO_3$ (Sigma), 0.1 g/l transferrin (Calbiochem), 0.25 g/l insulin (Sigma), 0.3 g/l L-glutamine (Gibco), and 10% fetal bovine serum) was replaced with growth medium (MEM (Gibco) containing 5 g/l glucose, 0.2 g/l $NaHCO_3$ (Sigma), 0.1 g/l transferrin (Calbiochem), 0.3 g/l L-glutamine (Gibco), 5% fetal bovine serum, 2% B-27 supplement (Gibco), and 2 μM cytosine arabinoside (Sigma)) 24–48 h after plating. Cultured neurons were transduced with recombinant lentiviruses and/or used for experiments as indicated.

Lentiviral vector production, transduction, and expression

Using a modified FUGW lentiviral vector (Lois *et al*, 2002; Pang *et al*, 2010), shRNA sequence against mouse SNAP-25 mRNA (GCAATGAGCTGGAGGAGATctcaagagaATCTCCTCCAGCTCATTGCT TTTTT; loop in lower case) was expressed using the H1 promoter, followed by mCherry expressed from the ubiquitin promoter. For overexpression studies, SNAP-25 cDNA was introduced into FUGW lentiviral vector (Lois *et al*, 2002) to generate N-terminally GFP-tagged WT SNAP-25. For the SNAP-25 truncation constructs, a stop codon was introduced in place of residue 198 or 181 to generate GFP–SNAP-25^{1-197} and GFP–SNAP-25^{1-180}. Lentiviral vector (containing shRNA or SNAP-25 variants), VSVG envelope glycoprotein and Δ8.9 HIV-1 packaging vectors were co-transfected (in a 1:1:1 molar ratio) into HEK293T cells (ATCC) in neuronal growth medium using Fugene-6 (Roche). Medium containing the viral particles was collected 48 h later and centrifuged for 10 min at 2000 r.p.m. to remove any cellular debris. The supernatant containing virions was added to cultured neurons at 5–7 DIV, and the expression of the recombinant proteins was monitored using mCherry or GFP fluorescence at 14 DIV before the beginning of the experiment.

Expression of SNAP-25 shRNA or GFP–SNAP-25 in mouse cortex

Medium containing lentiviral particles was harvested as described above, and the virions were concentrated by centrifugation at 50 000 g_{av} for 90 min. The viral pellet was re-suspended in neuronal medium (at 1/50 of the pre-centrifugation volume) containing 4 μg/ml polybrene (Sigma), snap-frozen in liquid N_2 and kept at −80°C. Heads of neonatal mouse pups (P1) were sterilized using Betadine (Purdue Pharma) and the pups were placed on ice for 1 min to anaesthetize them (while the thawed virus solution was warmed in the palm of the hand to body temperature). In all, 10 μl of the virus solution was injected into each cortex using a sterile Hamilton syringe (Davidson *et al*, 2010), feeling for the needle's passage through the soft skull. Pups were placed back with the mother immediately, and were monitored daily for negative effects of the injections (e.g. seizures, circling or paralysis, whereupon they would have been sacrificed). The injected animals were weaned at P19–21 and were transfusion fixed for brain histochemistry on P50.

Electrophysiology in cultured neurons

Whole-cell recordings in cultured neurons were conducted as described (Maximov *et al*, 2007). Briefly, cortical neurons were transferred from culture medium to extracellular solution (140 mM NaCl, 5 mM KCl, 2 mM $MgCl_2$, 2 mM $MgCl_2$, 10 mM HEPES-NaOH pH 7.4, 10 mM glucose) at room temperature. For recordings of evoked IPSCs, AMPA receptor and NMDA receptor blockers CNQX (20 μM) and D-AP-5 (50 μM) were added in the extracellular solution. To record mIPSCs, tetrodotoxin (TTX; 1 μM) was included in the extracellular solution in addition to CNQX and APV. For recordings of mEPSCs, TTX, APV, and $GABA_A$ receptor blocker picrotoxin (50 μM) were added to the extracellular solution. Patch pipette with resistance of 2.2–3.0 MΩ was filled with intracellular solution (135 mM CsCl, 10 mM HEPES, 1 mM EGTA, 1 mM Na-GTP, 4 mM Mg-ATP, and 10 mM QX-314, pH 7.4, adjusted with CsOH). Neurons were clamped at −70 mV. For evoked IPSC recording, synaptic current was evoked by 90 μA/1 ms current injections via a concentric bipolar electrode (CBAEC75, FHC) placed ~150 μm from the soma of patched neurons. The frequency, duration, and magnitude of the extracellular stimulus were controlled with a model 2100 Isolated Pulse Stimulator (A-M Systems) synchronized with Clampex 10.2 data acquisition software (Molecular Devices). To measure the size of readily releasable pool of synaptic vesicles, CNQX (20 μM), D-AP-5 (50 μM) and TTX were included in the extracellular solution and 0.5 M of sucrose were puffed by Picospritzer III (Dual channel, Parker) onto the recorded neurons for 30 s to evoke the release of readily releasable synaptic vesicles. Synaptic currents were monitored with a Multiclamp700B amplifier (Molecular Devices), sampled at 10 kHz and analysed offline using Clampfit 10.2 (Molecular Devices) software.

Behavioural and survival studies

Righting reflex (Chandra *et al*, 2005) was used to assess the level of paresis/paralysis. The mouse was held from tail and forced to lie down on one side. The mouse was recorded as paralyzed if it did not become upright within 5 s. Survival was recorded to the humane end point of study when the mouse became unable to reach food and water due to paralysis.

Immunofluorescence and immunohistochemistry

Cultured neurons infected with lentiviruses encoding GFP only, GFP–SNAP-25 WT, or the truncated versions GFP–SNAP-25^{1-197} and GFP–SNAP-25^{1-180} were washed three times with PBS, and fixed for 20 min at room temperature in PBS containing 4% paraformaldehyde. Following three washes with PBS, the fixed cultures were permeabilized for 15 min in blocking solution (PBS containing 3% BSA (Sigma)) supplemented with 0.1% Triton X-100 (Sigma). Synapsin antibodies (E028, polyclonal, 1:1000) and MAP2 antibodies (Sigma; monoclonal, 1:1000) were used as a synaptic and dendritic marker, followed by anti-rabbit Alexa 633 and anti-mouse Alexa 546 secondary antibody (1:500 each), both incubated for 1 h each in blocking solution. The coverslips were rinsed six times with PBS, mounted on slides in Vectashield aqueous mounting medium (Vector Labs) and stored at 4°C. Laser scanning confocal microscopy was performed to compare localization, with serial excitation at 633, 546, and 488 nm (for GFP), on a Leica TCS SP-2 inverted microscope.

For immunohistochemical studies, anaesthetized mice were perfused with ice-cold 4% paraformaldehyde in PBS, followed by removal of the brain and overnight fixation in 4% paraformaldehyde in PBS (room temperature). Fixed brains were cryopreserved in 30% sucrose in PBS for 2 days and frozen in Tissue Tek OCT embedding medium (Sakura Finetechnical). Sagittal brain sections (20 μm) were cut at −20°C (Leica CM3050S cryostat) picked up on slides and heat adhered at 37°C for 30 min. For immunostaining, slides were incubated in blocking solution (3% BSA, 0.1% Triton X-100 in PBS) for 1 h followed by overnight incubation with primary antibodies (4°C). Slides were washed three times in PBS (5 min each) and incubated in blocking buffer containing Alexa Fluor 488-, 546-, or 633-coupled secondary antibodies (Molecular Probes) for 3 h at room temperature. Following six washes in PBS, slides were mounted with Vectashield hard-set mounting medium with DAPI (Vector) followed by fluorescence microscopy.

All quantitations of immunofluorescence images were done with the image processing and analysis software ImageJ (NIH, Bethesda). Image acquisition and thresholding parameters were kept constant across each experiment.

Immunoblotting and immunoprecipitations

Either brain homogenates or cultured neurons were solubilized in 50 mM Tris–Cl buffer (pH 7.4) containing 150 mM NaCl and 0.1% Triton X-100. Following centrifugation at 16 000 g_{av} for 10 min at 4°C, the clarified lysate was used for immunoblotting (after addition of 2 × SDS sample buffer containing 10% β-mercaptoethanol) or subjected to immunoprecipitation. Immunoprecipitation was performed with the indicated primary antibodies and 30 μl of a 50% slurry of protein-G sepharose beads (Amersham) for monoclonal IgG, or protein-A sepharose beads (GE Healthcare) for polyclonal rabbit sera, for 2 h at 4°C. Control immunoprecipitations were performed with brain lysates with no antibody (for monoclonal antibodies), or with pre-immune serum (for polyclonal rabbit sera). Following five washes with 1 ml of the extraction buffer, bound proteins were eluted with 2 × SDS sample buffer containing 10% β-mercaptoethanol and boiled for 15 min at 100°C. Co-precipitated proteins were separated by SDS–PAGE, with 5–10% of the input in the indicated lane.

Protein quantitation

All quantitative immunoblotting experiments were performed with iodinated secondary antibodies as described (Rosahl *et al*, 1995). Samples were separated by SDS–PAGE, and transferred onto nitrocellulose membranes. Blots were blocked in Tris-buffered saline containing 0.1% Tween-20 (Sigma) and 5% fat-free milk for 2 h at room temperature. The blocked membrane was incubated in blocking buffer containing primary antibody for 1 h, followed by 3–5 washes. The washed membrane was incubated in blocking buffer containing either horseradish peroxidase (HRP)-conjugated secondary antibody (MP Biomedicals, 1:8000) for 2 h at room temperature, or ^{125}I-labelled secondary antibody (Perkin-Elmer, 1:1000) overnight at room temperature. HRP immunoblots were developed using enhanced chemiluminescence (GE Healthcare). ^{125}I blots were exposed to a phosphorimager screen (Amersham) for 1–7 days and scanned using a Storm scanner (GE Healthcare), followed by quantification with ImageQuant software (GE Healthcare).

Antibodies

Monoclonal antibodies. β-Actin (A1978, Sigma), clathrin (cl. 57.4, SYSY), rab3 (cl. 42.4, SYSY), GDI (cl. 81.2, SYSY), glycine receptor (146111, SYSY), GFAP (MAB360, Millipore), NSF (*N*-ethylmaleimide-sensitive factor) (cl. 83.1, SYSY), Hsc70 (cl. 3C5, SYSY), PSD95 (MA1046, Thermo), NeuN (MAB377, Millipore), rab5 (cl. 621.3, SYSY), synaptophysin (cl. 72.2, SYSY), α-SNAP (cl. 77.1, SYSY), SNAP-25 (SMI81, Sternberger Monoclonals; cl. 71.1, SYSY), synaptobrevin-2 (cl. 69.1, SYSY), synaptotagmin-1 (cl. 604.1, SYSY), syntaxin-1 (HPC1, SYSY), α-synuclein (610786, BD-Transduction), tau (MAB361, Millipore).

Polyclonal antibodies. Amphiphysin (P924), AP180 (155002, SYSY), cleaved caspase-3 (9661S; Cell Signaling), CD11 (ab75476; Abcam), complexin 1,2 (122002, SYSY), dynamin-1 (E026), GABA receptor (06-868, Upstate), Hsc70 (A903), MAP2 (AB5622, Millipore), NSF (J372), SGT (CHAT33), αSNAP (J373), SNAP-25 (P913), synaptobrevin-2 (P939), synaptojanin-1 (R323), synapsin (E028), syntaxin-1 (438B), α-synuclein (T2270), vGaT (131013, SYSY), vGluT1 (135302, SYSY).

mRNA isolation and quantitative RT–PCR

For quantitation of mRNA from mice, the brains were dissected and kept at 4°C in RNAlater solution (Ambion) and homogenized in Trizol solution (Invitrogen). RNA was extracted using the guanidinium salt/phenol–chloroform method (Chomczynski, 1993). RNA in the aqueous phase was isopropanol precipitated, followed by DNase I treatment (Qiagen) and LiCl precipitation. cDNA was prepared using oligo dT (16 nucleotides) and the Omniscript reverse transcription kit (Qiagen). Quantitative RT–PCR was performed using cross-intronic SNAP-25 primers (forward: CTGGCTGATGAGT CCCTGGAAAGC ACCC; reverse: TCCCGGGCATCATTTGTTACCCTG CGG), with BiP primers as control (forward: TACACTTGGTATTGA AACTG; reverse: GGTGGCTTTCCAGCCATT), and SYBR green 10 × Mastermix (Applied Biosystems). Quantitative PCR reaction and quantification, including water controls and melting curves to verify product specificity, were performed on HT-7500 thermocycler (Applied Biosystems) and visualized with SDS 2.0 software (Applied Biosystems).

For quantitation of mRNA from cortical cultures, neurons were lysed and total RNA was extracted and purified with RNAqueous-Micro kit (Ambion). mRNA level of individual genes was then analysed by one-step quantitative RT–PCR system with pre-made TaqMan gene expression assays (Applied Biosystems). Briefly, 30 ng of RNA sample in 1 μl volume was mixed with 10 μl of TaqMan fast universal PCR master mix (2 ×), 0.1 μl of reverse transcriptase (50 units/μl), 0.4 μl of RNase inhibitor (20 units/μl), 7.5 μl of H_2O, and 7 μl of TaqMan gene expression assay for the target gene (including the forward and reverse primers and the TaqMan FAM-MGB probe). The reaction mixture was loaded onto ABI7900 fast RT–PCR machine for 30 min of reverse transcription at 48°C followed by 40 PCR amplification cycles consisting of denaturation at 95°C for 1 s, annealing and extension at 60°C for 20 s. The amplification curve was collected and analysed with ΔΔCt methods for relative quantification of mRNAs. The amount of mRNA of target genes, normalized to that of an endogenous control and relative to the calibrator sample is calculated by $2^{-\Delta\Delta Ct}$. In the current study, glyceraldehyde 3-phosphate dehydrogenase (GAPDH) was used as the endogenous control. The TaqMan gene expression assays used in this study with SNAP-25 probe, IDMm00456921-m1.

Statistical analyses

Prism software (Graph Pad) was used to plot the survival and righting reflex curves, followed by Log-rank (Mantel–Cox) and Gehan–Breslow–Wilcoxon (not shown) tests to assess the statistical significance. Curves from electrophysiological studies (stimulation trains) were analysed by two-way repeated-measures ANOVA, also

using Graph Pad Prism. All other data shown are mean values ± s.e.m., and were analysed by Student's unpaired two-tailed *t*-test to compare the data groups.

Supplementary data

Supplementary data are available at *The EMBO Journal* Online (http://www.embojournal.org).

Acknowledgements

We thank Jason Mitchell, Andrea Roth, and Izabella Kornblum for technical assistance. This work was supported by a grant from the National Institute on Aging (NIH Grant RC2AG036614 to TCS), and fellowships from the Human Frontiers Program (LT00527/2006-L to MS) and the German National Academy of Sciences Leopoldina (BMBF-LPD 9901/8-161 to JB).

Author contributions: MS and TCS designed the study. MS, JB, PB, YZ, and WX performed and analysed the experiments. MS, JB, and TCS wrote the manuscript.

Conflict of interest

The authors declare that they have no conflict of interest.

References

Bronk P, Deák F, Wilson MC, Liu X, Südhof TC, Kavalali ET (2007) Differential effects of SNAP-25 deletion on Ca2 + -dependent and Ca2 + -independent neurotransmission. *J Neurophysiol* **98:** 794–806

Buchner E, Gundersen CB (1997) The DnaJ-like cysteine string protein and exocytotic neurotransmitter release. *Trends Neurosci* **20:** 223–227

Burre J, Sharma M, Tsetsenis T, Buchman V, Etherton MR, Sudhof TC (2010) Alpha-synuclein promotes SNARE-complex assembly *in vivo* and *in vitro*. *Science* **329:** 1663–1667

Chamberlain LH, Burgoyne RD (1997) The molecular chaperone function of the secretory vesicle cysteine string proteins. *J Biol Chem* **272:** 31420–31426

Chamberlain LH, Burgoyne RD (2000) Cysteine-string protein: the chaperone at the synapse. *J Neurochem* **74:** 1781–1789

Chandra S, Gallardo G, Fernandez-Chacon R, Schluter OM, Sudhof TC (2005) Alpha-synuclein cooperates with CSPalpha in preventing neurodegeneration. *Cell* **123:** 383–396

Chomczynski P (1993) A reagent for the single-step simultaneous isolation of RNA, DNA and proteins from cell and tissue samples. *Biotechniques* **15:** 532–534, 536–537

Davidson S, Truong H, Nakagawa Y, Giesler Jr GJ (2010) A microinjection technique for targeting regions of embryonic and neonatal mouse brain *in vivo*. *Brain Res* **1307:** 43–52

Fernandez-Chacon R, Wolfel M, Nishimune H, Tabares L, Schmitz F, Castellano-Munoz M, Rosenmund C, Montesinos ML, Sanes JR, Schneggenburger R, Sudhof TC (2004) The synaptic vesicle protein CSP alpha prevents presynaptic degeneration. *Neuron* **42:** 237–251

Galvin JE, Lee VM, Trojanowski JQ (2001) Synucleinopathies: clinical and pathological implications. *Arch Neurol* **58:** 186–190

Garcia-Junco-Clemente P, Cantero G, Gomez-Sanchez L, Linares-Clemente P, Martinez-Lopez JA, Lujan R, Fernandez-Chacon R (2010) Cysteine string protein-alpha prevents activity-dependent degeneration in GABAergic synapses. *J Neurosci* **30:** 7377–7391

Huang X, Wheeler MB, Kang YH, Sheu L, Lukacs GL, Trimble WS, Gaisano HY (1998) Truncated SNAP-25 (1-197), like botulinum neurotoxin A, can inhibit insulin secretion from HIT-T15 insulinoma cells. *Mol Endocrinol* **12:** 1060–1070

Kramer ML, Schulz-Schaeffer WJ (2007) Presynaptic alpha-synuclein aggregates, not Lewy bodies, cause neurodegeneration in dementia with Lewy bodies. *J Neurosci* **27:** 1405–1410

Lois C, Hong EJ, Pease S, Brown EJ, Baltimore D (2002) Germline transmission and tissue-specific expression of transgenes delivered by lentiviral vectors. *Science* **295:** 868–872

Maximov A, Pang ZP, Tervo DG, Sudhof TC (2007) Monitoring synaptic transmission in primary cultured neurons using local extracellular stimulation. *J Neurosci Methods* **161:** 75–87

Nosková L, Stránecký V, Hartmannová H, Přistoupilová A, Barešová V, Ivánek R, Hulková H, Jahnová H, van der Zee J, Staropoli JF, Sims KB, Tyynelä J, Van Broeckhoven C, Nijssen PC, Mole SE, Elleder M, Kmoch S (2011) Mutations in DNAJC5, encoding cysteine-string protein alpha, cause autosomal-dominant adult-onset neuronal ceroid lipofuscinosis. *Am J Hum Genet* **89:** 241–252

Pang ZP, Cao P, Xu W, Südhof TC (2010) Calmodulin controls synaptic strength via presynaptic activation of calmodulin kinase II. *J Neurosci* **30:** 4132–4142

Rosahl TW, Spillane D, Missler M, Herz J, Selig DK, Wolff JR, Hammer RE, Malenka RC, Südhof TC (1995) Essential functions of synapsins I and II in synaptic vesicle regulation. *Nature* **375:** 488–493

Rubinsztein DC (2006) The roles of intracellular protein-degradation pathways in neurodegeneration. *Nature* **443:** 780–786

Scheff SW, Price DA, Schmitt FA, DeKosky ST, Mufson EJ (2007) Synaptic alterations in CA1 in mild Alzheimer disease and mild cognitive impairment. *Neurology* **68:** 1501–1508

Schneggenburger R, Forsythe ID (2006) The calyx of Held. *Cell Tissue Res* **326:** 311–337

Sharma M, Burre J, Sudhof TC (2011) CSPalpha promotes SNARE-complex assembly by chaperoning SNAP-25 during synaptic activity. *Nat Cell Biol* **13:** 30–39

Tang J, Maximov A, Shin OH, Dai H, Rizo J, Sudhof TC (2006) A complexin/synaptotagmin 1 switch controls fast synaptic vesicle exocytosis. *Cell* **126:** 1175–1187

Tao-Cheng JH, Du J, McBain CJ (2000) Snap-25 is polarized to axons and abundant along the axolemma: an immunogold study of intact neurons. *J Neurocytol* **29:** 67–77

Tobaben S, Thakur P, Fernandez-Chacon R, Südhof TC, Rettig J, Stahl B (2001) A trimeric protein complex functions as a synaptic chaperone machine. *Neuron* **31:** 987–999

Umbach JA, Zinsmaier KE, Eberle KK, Buchner E, Benzer S, Gundersen CB (1994) Presynaptic dysfunction in Drosophila csp mutants. *Neuron* **13:** 899–907

Washbourne P, Thompson PM, Carta M, Costa ET, Mathews JR, Lopez-Bendito G, Molnar Z, Becher MW, Valenzuela CF, Partridge LD, Wilson MC (2002) Genetic ablation of the t-SNARE SNAP-25 distinguishes mechanisms of neuroexocytosis. *Nat Neurosci* **5:** 19–26

Wishart TM, Parson SH, Gillingwater TH (2006) Synaptic vulnerability in neurodegenerative disease. *J Neuropathol Exp Neurol* **65:** 733–739

Yang Y, Xia Z, Liu Y (2000) SNAP-25 functional domains in SNARE core complex assembly and glutamate release of cerebellar granule cells. *J Biol Chem* **275:** 29482–29487

Yankner BA, Lu T, Loerch P (2008) The aging brain. *Annu Rev Pathol* **3:** 41–66

Zinsmaier KE, Bronk P (2001) Molecular chaperones and the regulation of neurotransmitter exocytosis. *Biochem Pharmacol* **62:** 1–11

Zinsmaier KE, Eberle KK, Buchner E, Walter N, Benzer S (1994) Paralysis and early death in cysteine string protein mutants of Drosophila. *Science* **263:** 977–980